C. R. Palevol 15 (2016) 103–114

Contents lists available at ScienceDirect

Comptes Rendus Palevol

www.sciencedirect.com

General, Palaeontology, Systematics and Evolution (Palaeohistology – Bone histology)

The discrepancy between morphological and microanatomical patterns of anamniotic stegocephalian postcrania from the Early Permian Briar Creek Bonebed (Texas)

Distinction entre configurations morphologiques et micro-anatomiques du post-crâne de Stégocéphale anamniotique du Permien inférieur du gisement d'ossements de Briar Creek (Texas)

Dorota Konietzko-Meier[a,*,b], Christen D. Shelton[a,c], P. Martin Sander[a]

[a] *Division of Paleontology, Steinmann Institute, University of Bonn, Nussallee 8, 53115 Bonn, Germany*
[b] *Department of Biosystematics, University of Opole, Oleska 22, 45052 Opole, Poland*
[c] *Department of Zoology, University of Cape Town, Private Bag X3, Rhodes Gift, 7700 Rondebosch, South Africa*

ARTICLE INFO

Article history:
Received 29 January 2015
Received in revised form 2 June 2015
Accepted after revision 3 June 2015
Available online 11 August 2015

Handled by Michel Laurin

Keywords:
Early Permian
Briar Creek Bonebed
Histology
Long bones
Eryops
Archeria
Diadectes

ABSTRACT

The histological framework of thirteen Early Permian tetrapod long bones from a single locality, the Briar Creek Bonebed in Archer County, Texas, USA, is described from a series of transverse sections through the midshafts. The bones were morphologically categorized and belong to one of three taxa: *Eryops*, *Archeria*, and *Diadectes*. However, five histotypes are recognized. The first category includes the juvenile bone. The second histotype is characterized by the presence of radial vascular canals. The third histotype is characterized by the numerous longitudinal canals arranged in regular rows. In the fourth histotype, there is strong remodeling in the deep part of the cortex, creating a distinct border with the external layer of lamellar bone. In the fifth histotype, the deep part of the cortex is progressively remodeled towards osteoporosis with distinct layers of large circumferentially arranged erosion cavities. For femora and humeri, histotypes match morphology. Histotype II is characteristic for *Diadectes* propodials, histotype III is characteristic for *Eryops* propodials, and histotype IV is characteristic for *Archeria* propodials. A discrepancy between morphology and histology is observed in the ulnae, fibula and radius. This discrepancy may be explained by interspecific or intraspecific variability.

Mots clés :
Permien inférieur
Gisement d'ossements de Briar Creek
Histologie

RÉSUMÉ

Le cadre histologique de 13 os longs du Permien inférieur en provenance d'un site unique, le gisement d'ossements de Briar Creek d'Archer County, Texas, USA, est décrit à partir d'une série de coupes transversales au travers des diaphyses d'os. Les os sont rangés par catégorie morphologique et appartiennent à l'un des trois taxons *Eryops*, *Archeria* et *Diadectes*.

* Corresponding author.
E-mail address: dorotam@uni.opole.pl (D. Konietzko-Meier).

http://dx.doi.org/10.1016/j.crpv.2015.06.005
1631-0683/

Os longs
Eryops
Archeria
Diadectes

Cependant, on peut distinguer cing histotypes. La première catégorie comporte l'os juvénile ; la deuxième est caractérisée par la présence de canaux vasculaires radiaux ; le troisième histotype présente de nombreux canaux longitudinaux organisés en rangées régulières. Dans le quatrième histotype, il y a un remaniement intense dans la partie profonde du cortex, créant une bordure distincte avec un feuillet externe d'os lamellaire. Dans le cinquième histotype, la partie profonde du cortex est progressivement remaniée en direction de l'ostéoporose, avec des feuillets distincts constitués de grandes cavités d'érosion, disposées de manière circulaire. Pour les fémurs et les humérus, les histotypes correspondent à la morphologie. L'histotype II est caractéristique des propodiales de *Diadectes*, l'histotype III, des propodiales d'*Eriops*, et l'histotype IV, des propodiales d'*Archeria*. Une distinction entre morphologie et histologie et observée dans les ulna, fibula et radius. Cette distinction peut être expliquée par une variabilité interspécifique ou intraspécifique.

1. Introduction

The most extensive fossil record of Early Permian tetrapods is in the southwestern United States, specifically Texas and Oklahoma. The Texas material is mostly concentrated in and around the Archer County area (Fig. 1). Evidence of Early Permian vertebrates of both terrestrial and aquatic lifestyles has been collected from the famous Texas redbeds for over a century (Case, 1915; Cope, 1878; Romer, 1928, 1957; Sander, 1987, 1989; Shelton et al., 2013). One of the most important localities in the redbeds is the Briar Creek Bonebed, discovered by E.C. Case in 1912 (Case, 1915). Romer (1928) provided a comprehensive review of the fauna of this locality, listing the temnospondyls *Trimerorhachis* sp., *Zatrachys serratus*, *Eryops* sp., and *Aspidosaurus* sp., the lepospondyl *Diplocaulus* sp., the anthracosaur *Archeria* sp. (formerly *Cricotus* sp.), the diadectomorph *Diadectes* sp., the parareptile *Bolosaurus* sp., and the synapsids *Dimetrodon* sp., *Edaphosaurus* sp., and *Ophiacodon* sp.

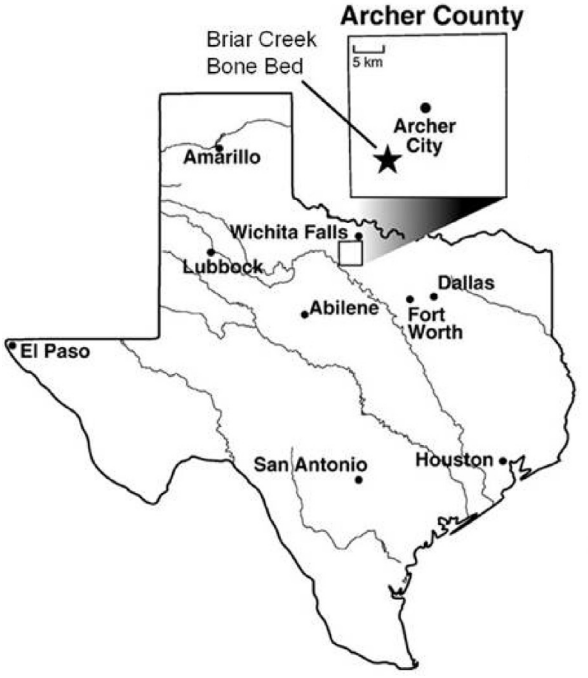

Fig. 1. Location of Archer County, Texas, USA. This map shows the location of the Briar Creek Bonebed, the site of the 2010 and 2011 excavations that yielded the material for this study. This bonebed is in the Nocona Formation (Lower Permian, Artinskian).
Fig. 1. Localisation d'Archer County, États-Unis. La carte indique la localisation du gisement d'ossements de Briar Creek, le site des fouilles de2010 et 2011 qui ont fourni le matériel de l'étude ici présentée. Le lit qui contient les os se trouve dans la formation Nocona (Permien inférieur, Artiskien). Modifié d'après Labandeira et Allen (2007).
Modified from Labandeira and Allen (2007).

The non-amniote bones reported here belong to large stegocephalians, which can grow up to two meters in length: *Eryops*, *Archeria*, and *Diadectes*, representing various lifestyles and phylogenetic positions among early Tetrapoda.

Of particular interest is the iconic temnospondyl *Eryops*, whose habitat preference has been debated. Case (1915) considered *Eryops* an aquatic animal based on the dorsal position of its nostrils and orbits. Conversely, Romer (1947) and Pawley and Warren (2006) argued that *Eryops* was a terrestrial animal because of its well-ossified limbs (including a well-ossified carpus and tarsus) and a highly ossified vertebral column. Despite the well-ossified skeleton, the spongy structure observed in the long bones of *Eryops* resembles that of aquatic animals (Quémeneur et al., 2013; Ricqlès and Buffrénil, 2001; Sanchez et al., 2010). Sanchez et al. (2010) pointed out that high torsional resistance of the long bones suggested that *Eryops*, even though hypothesized to have mostly dwelt on lake bottoms, may have had the ability to venture into the terrestrial environment.

Archeria was an elongate aquatic predatorial anthracosaur (Romer, 1957). Some authors (Laurin and Reisz, 1997; Marjanović and Laurin, 2013) placed embolomeres among stem-tetrapods, rather than in their traditional position in Reptiliomorpha (e.g. Ruta et al., 2003), so the affinities of embolomeres are currently contentious.

The bone histology of the *Archeria* femur midshaft was illustrated by de Ricqlès (1975, 1978). According to these papers, the cortex is highly remodeled, resembling Haversian bone (Ricqlès, 1978), and the medullary region is filled with spongiosa (Ricqlès, 1978).

Diadectes belongs to Diadectomorpha, which is generally placed as the sister taxon to the crown amniotes (sauropsids + synapsids), together forming

the monophyletic Cotylosauria sensu Laurin (e.g. Laurin, 2004; Laurin and Reisz, 1995; Ruta et al., 2003). Based on dental and postcranial anatomy, members of Diadectidae are thought to represent the earliest known examples of vertebrates capable of processing high-fiber terrestrial plants (summarized in Kissel, 2010). *Diadectes* was a heavily built animal with a thickened skull, heavy vertebrae and ribs, massive limb girdles but short, robust limbs, all of which are suggestive of a terrestrial life style. Ricqlès (1974) described *Diadectes* histology from a femoral diaphysis. His findings showed that the cortex consisted of lamellar bone matrix with dense longitudinal vascular canals.

The main goal of this study is to provide the first histological description of various non-amniotic tetrapod long bones from classical Early Permian taxa, only briefly described previously (Quémeneur et al., 2013; Ricqlès, 1974, 1975, 1978, Sanchez et al., 2010), and to test if the histological framework is consistent with taxonomy. A detailed analysis of the biology of the taxa discussed here, based on bone histology, is in progress and will be published separately.

2. Materials and methods

2.1. The Briar Creek Bonebed

The Briar Creek Bonebed (Case, 1915, spelled "Brier Creek") was reported to yield partial skeletons at best, but mostly isolated bones (Case, 1915; Romer, 1928). Teams from the University of Bonn under the leaderships of P.M. Sander and C.D. Shelton reopened the quarry in 2010 and 2011, collecting numerous bones, including those sampled for this study.

The bonebed is about 30 cm thick and consists of an accumulation of unsorted and disarticulated reptile and amphibian bones of variable preservation encased in a grey mudstone. Some bones have a heavy concretionary cover of ironstone. The Briar Creek Bonebed taphonomy is unique in that some of the bones are considered to have decomposed before preservation (Case, 1915). Case (1915) originally hypothesized that this area represented a pool or swamp that functioned as a macerating tank. The deposit could also have been an oxbow lake or swamp formed by the meandering of a river similar to the hypothesized paleoenvironment described by Sander (1989) for other Lower Permian bonebeds in Archer County. The isotope analyses indicate a non-marine origin of the localities from the Early to Middle Permian of the southwestern USA, including the Archer City Formation (Fischer et al., 2014).

2.2. Material

Thirteen long bones, mostly complete, recovered during the 2010 and 2011 excavations pertaining to different anamniotic stegocephalians were chosen for consumptive sampling (Table 1). All bones belong to the histological collection of the University of Bonn, Steinmann Institute, Germany (IPBSH).

2.3. Methods

Taxonomic determination – Taxonomic determination of the sampled bones was made by comparison with the literature on Early Permian tetrapod morphology (Case, 1911; Cope, 1878; Kissel, 2010; Miner, 1925; Pawley and Warren, 2006; Romer, 1957) and by personal studies of Lower Permian vertebrate collections curated in institutions in the United States undertaken by CDS. These include the Dallas Museum of Natural History (DMNH), the Museum of Comparative Zoology of Harvard University (MCZ), the Field Museum of Natural History in Chicago (FMNH), the Texas Memorial Museum (TMM) in Austin, TX, the Sam Noble Museum of Natural History at the University of Oklahoma in Norman, OK (OMNH), the American Museum of Natural History in New York City (AMNH), the University of Michigan Museum of Paleontology in Ann Arbor, MI (UMMP), and the Yale Peabody Museum of Natural History in New Haven, CT (YPM).

While *Archeria* was well described by Romer (1957) based on articulated skeletons from the Geraldine Bonebed, Archer County, Texas, regrettably there are no complete monographic descriptions of *Eryops* based on articulated specimens despite the exceptional preservation of several skeletons in the Geraldine Bonebed (Sander, 1987). Miner (1925) provided the description only of the pectoral limb of *Eryops*. Pawley and Warren (2006) redescribed the anatomy of *Eryops*, basing the descriptions on numerous isolated bones in various collections instead of on the articulated skeletons from the Geraldine Bonebed that are on exhibit in several North American museums (Sander, 1987).

Histological sections – All bones were sectioned transversely at or near the midshaft and reconstructed after cutting. The thin-sections were prepared according to standard petrographic methods (Lamm, 2014). Sections were ground and polished using wet SiC grinding powder (600 and 800 grit). The thin sections were then studied under a LEICA DMLP light microscope in normal and polarized transmitted light. Images of entire slides showing whole bone cross sections were produced with an Epson V740 PRO high resolution scanner.

The determination of histotypes – In order to test if the histological framework is consistent with taxonomy the sections were, independently of the taxonomic determination, sorted into histotypes based on the microanatomical and histological characters (character of primary tissue, vascular canals organization, degree of remodeling, growth marks). The histological terminology follows Francillon-Vieillot et al. (1990).

3. Results

3.1. Morphological description

Humerus – All humeri (Table 1) represent the basal tetrapod tetrahedral form with a relatively low degree of torsion in the shaft. The short, thick humeral shaft is somewhat laterally compressed, and roughly quadrangular in cross section. Specimens IPBSH-23 and IPBSH-48 display an

Table 1
Bones of anamniotic tetrapods from the Briar Creek Bonebed (Lower Permian, Texas) sampled for this study.
Tableau 1
Ossements de tétrapodes anamniotiques du Briar Creek bonebed (Permien inférieur, Texas) échantillonnées pour cette étude.

Col. num.IPBSH-	Bone	Length (mm)	M-taxon	Histotype	Figures
38	Humerus left	56	*Archeria*	IV	Fig. 6C, D
48	Humerus left	67	*Archeria*	IV	Fig. 6E, F
23	Humerus right	91	*Archeria*	IV	Not shown
74[a]	Ulna left	94	*Archeria*	V	Figs. 2C and 7
65	Femur left	87	*Archeria*	IV	Fig. 2F
68	Tibia right	58	*Archeria*	IV	Not shown
75[a]	Radius right	87	*Eryops*	V	Not shown
76	Ulna left	65	*Eryops*	I	Figs. 2A and 3A–C
73[a]	Ulna left	87	*Eryops*	IV	Figs. 2B and 6A, B and G, H
64	Femur right	113	*Eryops*	III	Not shown
78	Femur right	128	*Eryops*	III	Figs. 2D and 5
81[a]	Fibula right	127	*Eryops*	IV	Not shown
77	Femur left	138	*Diadectes*	II	Fig. 2E and 4

Col. num.: collection number; M-taxon: taxonomical determination of the bone based on the morphological characters.
[a] Observed a discrepancy between morphotype and histotype.

entepicondylar foramen that is unusual for temnospondyls. The most diagnostic bones are humeri IPBSH-48 and 23, having an expanded deltopectoral crest forming a highly developed flange which projects anteriorly. The anterior flange in the smallest specimen IPBSH-38 is not as distinctive as in IPBSH-23 and IPBSH-48. Based on this unique morphology of the deltopectoral crest all three bones were identified as *Archeria* (Romer, 1957).

Radius – The single radius in this study, IPBSH-75, is a stout element with flared proximal and distal ends. The distal portion is flattened in the extensor - flexor plane and broader than the proximal portion. The extensor surface is convex in transverse section, whereas the flexor surface is gently concave. A sharp-edged ventromesial radial ridge passes down the midline of the anterior surface. On the flexor surface, the ventral radial crest is located slightly medial to the posterior edge. The proximal articular surface is sub-rectangular whereas the distal articular surface is more triangular. The morphology of radius IPBSH-75 is indicative of *Eryops* (Miner, 1925; Pawley and Warren, 2006).

Ulna – The ulnae (Table 1) are relatively slender, and their shaft is anteroposteriorly flattened (Fig. 2A-C)

. The ulnar extensor keel has a rugosity on the proximal region, indicating the attachment to the triceps muscle (Fig. 2A). On the posterior surface, a low ulnar crest originates below the humeral articular surface and branches at the midpoint of the shaft into the posterolateral ulnar crest. In proximal view, the humeral articular surface is approximately quadrangular; only in ulna IPBSH-74 is it thinner. In specimens IPBSH-73 and IPBSH-74, the olecranon process is more ossified and raised like in IPBSH-76 (Fig. 2A–C). Ulnae IPBSH-76 and IPBSH-73 (Fig. 2A-B) both have a broad proximal head that is diagnostic of *Eryops* (Miner, 1925; Pawley and Warren, 2006). Ulna IPBSH-74 (Fig. 2C) has a flat humeral articular surface suggestive of an affinity with *Archeria* (Romer, 1957).

Femur – The four femora (Table 1) represent the plesiomorphic condition of Permo-Carboniferous tetrapods, essentially a stout cylinder with expanded ends and ventral structures associated with muscular attachments (Fig. 2D–F). As is typical of Permo-Carboniferous tetrapods, the proximal articular surface is a ribbon-shaped oval that extends anteroposteriorly, being relatively narrow dorsoventrally, convex in outline dorsally and concave ventrally. The distal articular face of the femur is triangular. The posterior fibular condyle is rectangular, and the distal articular facet of the femur is bisected on the dorsal side by the prominent intercondylar fossa (fossa tendinalis) and tibial condyle. On the ventral side, proximal to the posterior edge of the articular surface, the distal end of the adductor crest constitutes the apex of a triangle. The fossa poplitea is located anteriorly to the apex. The ventral surface of the femur possesses an intertrochanteric fossa, internal and fourth trochanters, a longitudinal adductor crest, and a concave popliteal space (Fig. 2D–F). The internal trochanter lies close to the head of the bone at the proximal end of a raised and thickened ridge. As the ridge continues distally along the trochanter, it descends into the general contours of the shaft, which bears a prominent pit and associated rugosities, perhaps representing the fourth trochanter.

Femora were taxonomically assigned (Fig. 2D–F) mostly based on the different shape of the proximal head and different architecture of adductor crests.

In femora IPBSH-64 and IPBSH-78, the anterior part of the proximal articular surface is somewhat thicker than the posterior part. Both bones have a very prominent adductor crest, which arises near the fourth trochanter, essentially in line with the base of the internal trochanter. The adductor crest slants distally across the shaft to terminate laterally at the ventral tip of the fibular articular surface. In femur IPBSH-78, the adductor crest bifurcates distally, enclosing the popliteal space. Based on these characters femora IPBSH-64 and IPBSH-78 (Fig. 2D) can be identified as *Eryops* (Pawley and Warren, 2006).

The exquisite preservation of IPBSH-77 (Fig. 2E) allowed the identification of morphological characters (the articular face of the proximal end is nearly flat and descends almost perpendicularly along the posterior, low adductor crest) that are diagnostic of *Diadectes* (Case, 1911).

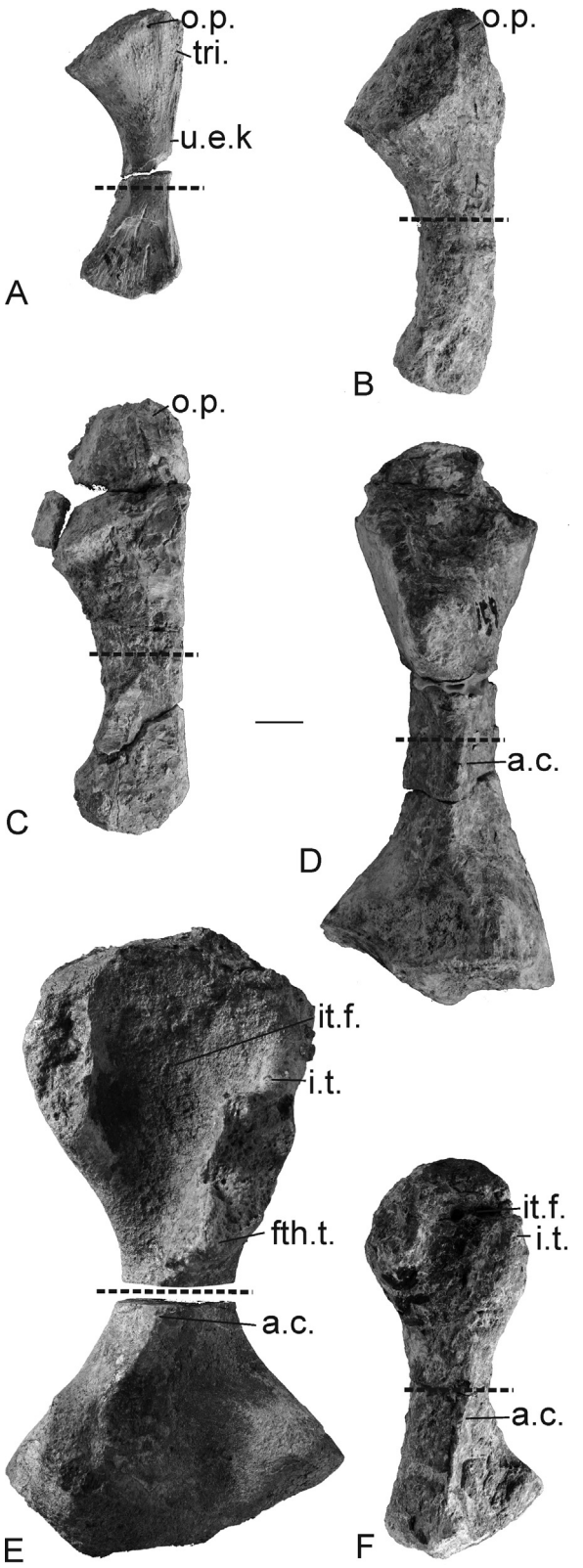

Fig. 2. The anamniotic tetrapod femora and ulnae from the Briar Creek Bonebed sectioned for this study and their taxononic identifications based on morphology. A. Left ulna IPBSH-76 of *Eryops*, in lateral view. B. Left ulna IPBSH-73 of *Eryops*, in lateral view. C. Left ulna IPBSH-74 of *Archeria*, in lateral view. D. Right femur IPBSH-78 of *Eryops*, in ventral view. E. Left femur IPBSH-77 of *Diadectes*, in ventral view. F. Left femur IPBSH-65 of *Archeria*, in ventral view. The scale bar is equal to 10 mm. The dotted lines indicate the section plane. Abbreviations: a.c.: adductor crest; i.t.: internal trochanter; it.f.: intertrochanteric fossa; fth.t.: fourth trochanter: o.p.: olecranon process; tri.: the attachment to the triceps muscle; u.e.k.: ulnar extensor keel.

In femur IPBSH-65 (Fig. 2F), difference in size between the anterior and posterior parts of the articular surface is slight. Femur IPBSH-65 with its massive proximal articular surface and low-reaching adductor crest belongs to *Archeria* (Romer, 1957).

Tibia – The single tibia in this study, IPBSH-68 (Table 1), is a slender bone with a gently expanded proximal head. The cnemial crest does not project sharply but rather it is a small rounded swelling at the extensor margin of the bone. The cnemial trough forms a shallow constriction on the extensor side of the femoral articular surface, marking the boundary between the anterior and posterior articular surfaces. The distal articular surface is more triangular, with a flattened flexor edge and strongly convex exterior side with continuous articulation facets to the fibula. The flexor surface bears a series of crests; however, the bone surface is poorly preserved so the morphological details are not obvious. Based on the morphology tibia IPBSH-68 belongs to *Archeria* (Romer, 1957).

Fibula – The single fibula in this study, IPBSH-81 (Table 1), has a slightly expanded and broadened head with a terminal articular surface for the femur, a flattened shaft, a broad proximal end, and a distal segment with a terminal surface for the articulation of the tarsus. In proximal view, the proximal surface twists at approximately 300 to the distal surface. The bone is strongly concave along its anterior (tibial) margin; the posterior edge is nearly straight. The articular surface for the femur is a crescentic oval, somewhat convex in outline along its extensor margin, concave on the opposite edge. The broad fibular extensor ridge bulges out from the femoral articular surface and distally passes directly down the proximal head on the extensor side. A short anterior fibular ridge is located on the anterior proximal surface. The flexor surface of the shaft is gently concave along its length. A deep fibular sulcus crosses the anterodistal corner. The shallow posterior fibular ridge runs along the posteromedial edge of the bone. Morphology of the fibula IPBSH-81 suggests an *Eryops* affinity (Pawley and Warren, 2006).

Fig. 2. Fémurs et ulnas de tétrapode anamniotique du lit ossifère de Briar Creek, sectionnés pour cette étude et leurs identifications taxonomiques basées sur la morphologie. A. Ulna gauche IPBSH-76 d'Eryops en vue latérale. B. Ulna gauche IPBSH-73 d'*Eryops* en vue latérale. C. Ulna gauche IPBSH-74 d'*Archeria* en vue latérale. D. Fémur droit IPBSH-78 d'*Eryops* en vue ventrale. E. Fémur gauche IPBSH-77 de *Diadectes* en vue ventrale. F. Fémur gauche IPBSH-65 d'*Archeria* en vue ventrale. La barre d'échelle est égale à 10 mm. Les lignes pointillées indiquent la section plane. Abréviations : a.c. : crête adductrice ; i.t. : trochanter interne ; it.f. : fosse inter-trochanters ; fth.t. : quatrième trochanter ; o.p. : processus de l'oléocrâne ; tri : attache au muscle triceps ; u.e.k. : extenseur de l'ulna.

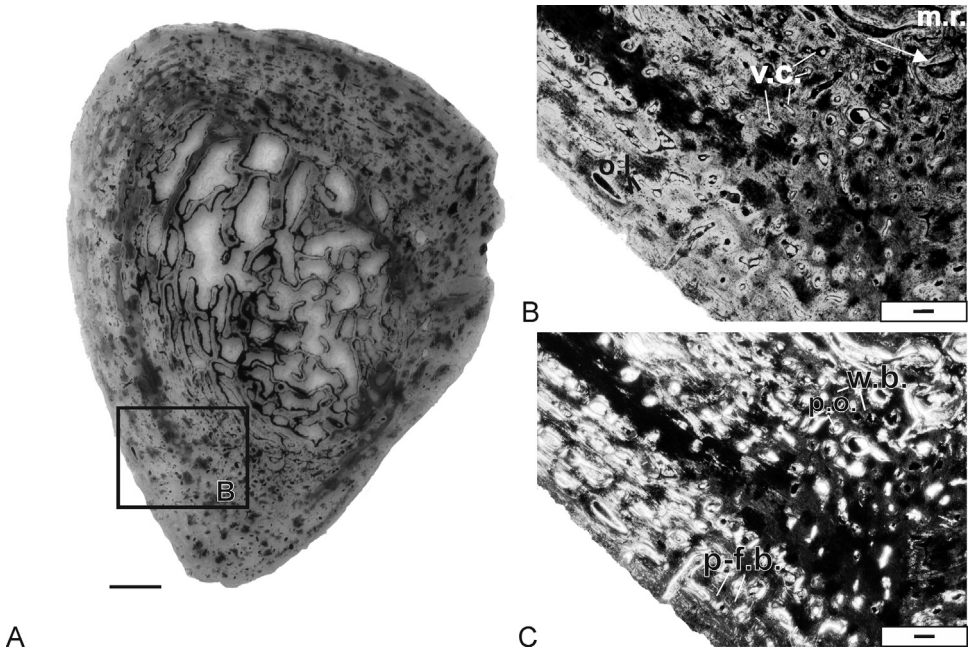

Fig. 3. Histotype I evident in ulna IPBSH-76 identified as *Eryops* based on morphology. A. Microanatomy of ulna IPBSH-76 midshaft. B. Close-up of A with regularly arranged rows of vascular canals, imaged in normal transmitted light. The white arrow indicates the remodeled medullary margin. C, the same as B, but in polarized transmitted light. Scale bars equal 100 μm for A and 200 μm for B and C. Abbreviations: m.r.: medullary region; p-f.b.: parallel-fibred bone; p.o.: primary osteon; o.l.: osteocyte lacunae; v.c.: vascular canal; w.b.: woven bone.

Fig. 3. Histotype I évident dans l'ulna IPBSH-76, identifié d'après la morphologie comme appartenant à *Eryops*. A. Microanatomie de l'ulna IPBSH-76 à diaphysaire. B. Agrandissement de A, avec des rangées régulièrement organisées de canaux vasculaires, en lumière transmise normale. La flèche blanche représente la marge médullaire remodelée. C. Idem B, mais en lumière transmise polarisée. Les barres d'échelle représentent 100 μm pour A et 200 μm pour B et C. Abréviations : m.r. : zone médullaire ; p-f.b. : os à fibres parallèles ; p.o. : ostéone primaire ; o.l. : lacunes d'ostéocyte ; v.c. : canal vasculaire ; w.b. : os fibreux.

3.2. Histological description

Five histotypes are recognized amongst the sampled long bones (Table 1).

Histotype I – This histotype is recognized in the smallest ulna (IPBSH-76; Table 1), based on the morphology assigned to *Eryops*. There are numerous vascular canals arranged in regular concentric rows (Fig. 3). The primary tissue is parallel-fibered and woven bone (Fig. 3C). There is a high number of osteocyte lacunae. Remodeling is concentrated at the medullary margin (Fig. 3B). No growth marks are present. This histological framework suggests an early ontogenetic stage, but it is not possible to narrow down the stage further. This is why we decided to treat the immature bone as a separate histotype.

Histotype II – Histotype II is only represented by femur IPBSH-77 (Fig. 4), which can be confidently assigned to *Diadectes*. The unremodeled cortex is relatively thin; the dorsal side consists of parallel-fibered bone, in the ventral region the tissue is more organized than the dorsal side. The remodeling of the cortex increases gradually towards the remodeled perimedullary region. There is no clear boundary between cortex and medullary region. The medullary region is large, with a few thickened trabeculae (Fig. 4A). This histotype has a diagnostic vascularization consisting of the slightly oblique, but clearly radially arranged vascular canals (Fig. 4B–C). The osteocyte lacunae are small, but numerous. Sharpey's fibers are only visible on the ventral side in the region of the adductor crest.

Histotype III – The primary tissue of this histotype, which is displayed in the femora that can confidently be assigned to *Eryops*, consists of lamellar or parallel-fibered bone. Longitudinal vascular canals are arranged in regular rows throughout the entire cortex, grading from simple vascular canals in the outer cortex to more primary osteons in the deeper cortex (Fig. 5A). The degree of remodeling increases from the bone periphery inwards from secondary osteons to erosion cavities (Fig. 5C). Between the rows of vascular canals are layers of a highly organized bone matrix with growth marks. In femur IPBSH-78, two to four growth lines in each annulus are visible (Fig. 5C). Throughout the entire section, the osteocyte lacunae are highly concentrated and circular in section (Fig. 5C). Sharpey's fibers are sparse, mostly present in the region of the adductor crest. The cortex transitions into the medullary region through the remodeled perimedullary region. However, the borders between the primary cortex, perimedullary region, and medullary space are relatively clear. The medullary region is occluded by a few thick trabeculae, but the central region remains empty.

Histotype IV – The tissue type is recognized by a thick, lamellar bone layer near the surface and is seen in bones (humeri, a femur and a tibia) that can confidently be assigned to *Archeria* (Fig. 6C–H); moreover, in the ulna

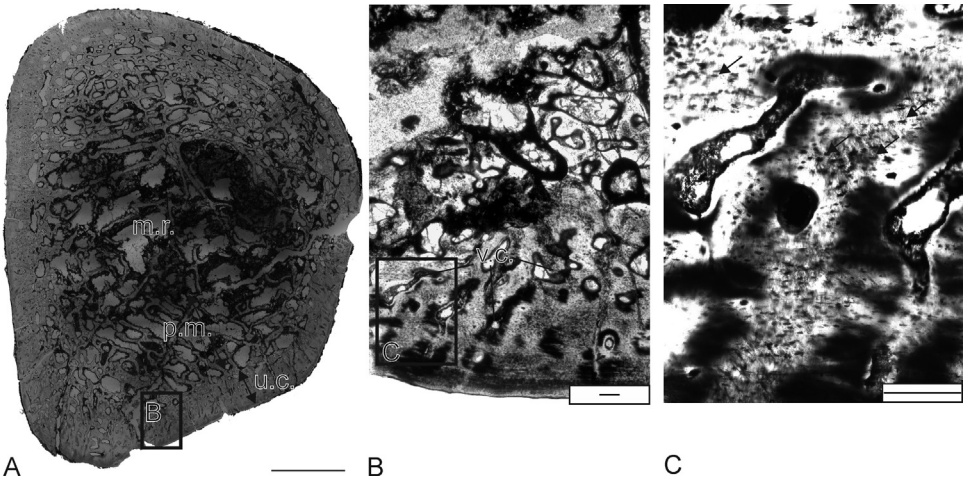

Fig. 4. Histotype II, represented by *Diadectes* femur IPBSH-77. A. The microanatomy of the midshaft. B. Histological details of the cortex vascularized by radial canals, imaged in normal transmitted light. C. Enlargement of a radial canal from B, imaged in normal transmitted light. Black arrows indicate the osteocyte lacunae. Scale bars equal 500 μm for A, and 200 μm for B and C. Abbreviations: m.r.: medullary region; p.m.: remodeled perimedullary region; u.c.: unremodelled cortex; v.c.: vascular canal.

Fig. 4. Histotype II, représenté par le fémur IPBSH-77 de *Diadectes*. A. Microanatomie de la diaphyse. B. Détails histologiques du cortex vascularisé par des canaux radiaux, en lumière transmise normale. C, Agrandissement d'un canal radial de B, en lumière transmise normale. Les flèches noires indiquent les lacunes d'ostéocytes. Barres d'échelle 500 μm pour A et 200 μm pour B et C. Abréviations : m.r. zone médullaire ; p.m. : zone péri-médullaire remodelée ; u.c. : cortex non remodelé ; v.c. : canal vasculaire.

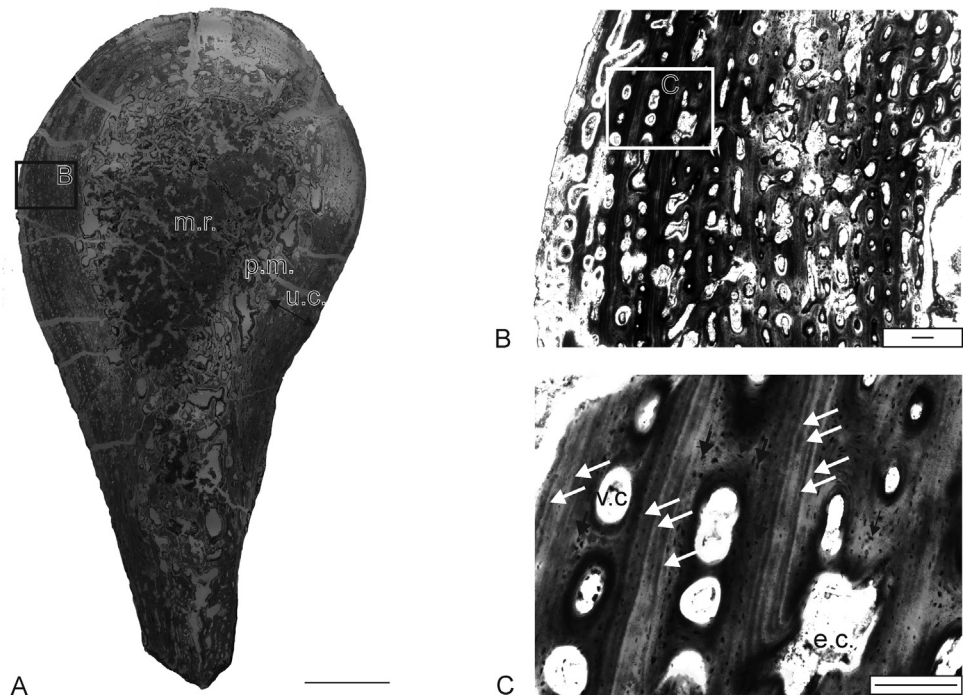

Fig. 5. Histotype III represented by *Eryops* femur IPBSH-78. A. The microanatomy of the midshaft. B. The histological details of the cortex. Note the regular rows of vascular canals. C. Growth lines (white arrows) visible in the annuli of the *Eryops* cortex, enlargement of B, imaged in normal transmitted light. Black arrows indicate the osteocyte lacunae. Scale bars equal 500 μm for A, and 200 μm for B and C. Abbreviations: e.c.: erosion cavity; m.r.: medullary region; p.m.: remodeled perimedullary region; u.c.: unremodelled cortex; v.c.: vascular canal.

Fig. 5. Histotype III représenté par le fémur d'*Eriops* IPBSH-78. A. Microanatomie de la diaphyse. B. Détails histologiques du cortex. À noter les rangées régulières de canaux vasculaires. C. Lignes de croissance (flèches blanches) visibles sur les anneaux du cortex d'*Eryops*, agrandissement de B, en lumière transmise normale. Les flèches noires indiquent les lacunes d'ostéocytes. Les barres d'échelle sont de 500 μm pour A et 200 μm pour B et C. Abréviations : e.c. : cavité d'érosion ; m.r. : zone médullaire ; p.m. : zone péri-médullaire remodelée ; u.c : cortex non remodelé ; v.c. : canal vasculaire.

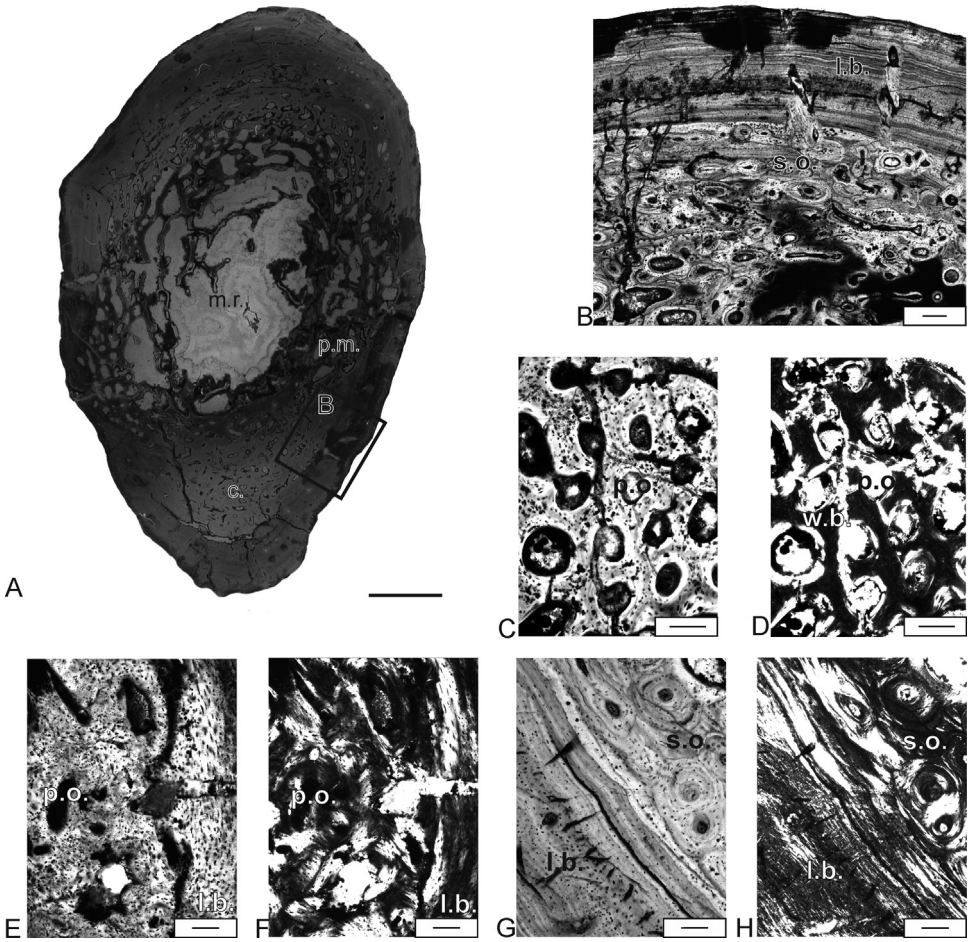

Fig. 6. Histotype IV, as seen in *Eryops*? ulna IPBSH-73 (A, B and G, H) and *Archeria* humeri IPBSH-38 and IPBSH-48 (C–F). A. The microanatomy of the ulna midshaft. B. The histological details of the cortex. Note the thick layer of compact bone and highly remodeled deep cortex, imaged in normal transmitted light. C. Primary osteons are visible in the cortex of humerus IPBSH-38, imaged in normal transmitted light. D. The same as C, but in polarized transmitted light. Note the woven bone between the primary osteons forming incipient fibrolamellar bone. E. Primary osteons are visible in the cortex of humerus IPBSH-48. Note the highly organized matrix, imaged in normal transmitted light. F, the same as E but in polarized transmitted light. G. Lamellar bone is present in outermost cortical layer, and the deeper cortex is highly remodeled deeper cortex. Note the distinct border between these layers, imaged in normal transmitted light. H. The same as G but in polarized transmitted light. Scale bars equal 500 μm for A, 200 μm for B, and 100 μm for C–H. Abbreviations: c.: cortex; l.b.: lamellar bone; m.r.: medullary region; p.m.: remodeled perimedullary region; p.o.: primary osteon; s.o.: secondary osteon; w.b.: woven bone; v.c.: vascular canal.

Fig. 6. Histotype IV, comme vu dans l'ulna IPBSH-73 d' *Eryops* ? (A, B et G, H) et dans les humérus IPBSH638 et IPBSH-48 d'*Archeria* (C–F). A. Microanatomie de la diaphyse de l'ulna. B. Détails histologiques du cortex. A noter le feuillet épais d'os compact et le cortex profond intensément remodelé, en lumière transmise normale. C. Ostéones primaires visibles dans le cortex de l'humérus IPBSH-38 en lumière transmise normale. D. Idem C, mais en lumière transmise polarisée. A noter l'os fibreux entre les ostéones primaires formant le début d'un os fibro-lamellaire. E. Ostéones primaires visibles dans le cortex de l'humérus IPBSH-48. À noter la matrice très organisée en image transmise normale. F. Idem E, mais en lumière transmise polarisée. G. Os lamellaire dans le feuillet cortical le plus externe et cortex profond très remodelé. À noter la limite distincte entre ces feuillets en lumière transmise normale. Les barres d'échelle sont de 500 μm pour A, 200 μm pour B et 100 μm pour C–H. Abréviations : c. : cortex ; l.b. : os lamellaire ; m.r. : zone médullaire ; p.o. : ostéone primaire ; s.o. : ostéone seondaire ; w.b. : os fibreux ; v.c. : canal vasculaire.

(IPBSH-73) and fibula (IPBSH-81), both have a morphology diagnostic of *Eryops* (Table 1, Fig. 6A and B). There is a sharp contrast between the borders of the primary lamellar layer and the highly vascularized remodeled cortex (Fig. 6B). The degree of remodeling here depends on the size of the bone. In humerus IPBSH-38, dense vascularization is mostly simple canals with the deposition of primary lamellar bone in some vascular canals; small patches of incipient fibrolamellar bone (FLB) are also present (Fig. 6C–D). Primary osteons dominate the cortex of humerus IPBSH-48 (Fig. 6E–F), whereas humerus IPBSH-23, ulna IPBSH-73, tibia IPBSH-68, and fibula IPBSH-81 mostly show secondary osteons (Fig. 6G–H). In femur IPBSH-65, two vascularized layers separated by an avascular layer are present. The outer layer is composed of primary osteons and the inner layer is composed of secondary osteons deeper in the cortex. This region of the cortex gradually transitions to the medullary region with thick trabeculae (Fig. 6A). The perimedullary region was created by the extensive remodeling of the medullary region, which is open in the center

(Fig. 6A). The osteocyte lacunae in the avascular layers are dense and flattened; they are more circular in the vascularized regions. The presence of Sharpey's fibers is extensive throughout the section.

Histotype V – A highly porous cortex is present in two bones, ulna IPBSH-74 and radius IPBSH-75, which morphologically belong to *Archeria* and *Eryops*, respectively. The outermost layer of these bones consists of thin lamellar bone (Fig. 7A). The vascular canals are visible only next to the lamellar layer. The larger part of the cortex is highly porous, resembling spongy bone with regular thin trabeculae consisting of primary and secondary tissue (Fig. 7B–D). No growth marks are preserved. In the central part of the sections, there is an open medullary cavity. Osteocyte lacunae are numerous and spindle-shaped. Extensive Sharpey's fibers are visible through the primary cortex.

4. Discussion

4.1. Discrepancy between morphology and histology

The previous description of the faunal content of the Briar Creek Bonebed provided by Romer (1957) and the morphological characters of these bones limit the probable identity of the potential taxa to three well known genera: *Eryops*, *Archeria*, and *Diadectes* (Table 1). However the histological variation visible among the studied bones is higher. The bones based on the morphology assigned to *Archeria* represent two histotypes (IV and V). The *Eryops* bones show higher variability and represent the histotypes I, III, IV and V (Table 1). For humeri and femora, the histotype seems to be directly related to the taxon. Histotype II is diagnostic of *Diadectes*, histotype III of *Eryops*, and histotype IV of *Archeria* (Figs. 4-6, Table 1). That pattern is not observed in the ulnae, fibula and radius. These bones do not repeat the histological framework visible in the propodials representing the new histotypes (I and V) or the histotypes known from femora, but assigned to different taxa. Both large ulnae are similar in length, but show a discrepancy between morphology and histology (Table 1). Ulna IPBSH-73 (Fig. 2B), which is assigned to *Eryops* based on morphology, shows histotype IV (Fig. 6A-B, Table 1), diagnostic of *Archeria* in propodials. The flat humeral articular surface of ulna IPBSH-74 suggests that this bone belongs to *Archeria* (Fig. 2C), but it shows histotype V (Fig. 7), not seen in any propodials. Moreover, the second bone with histotype V (radius IPBSH-75) morphologically resembled *Eryops*. Fibula IPBSH-81 represents histotype IV, but morphologically it is slender and not as broad distally as described by Romer (1957) for *Archeria*.

4.2. The origin of the variability

Specimens morphologically identified as *Eryops* show four different histotypes, and morphologically *Archeria* bones represent two histotypes (Table 1).

There are several potential explanations for this histotype variability: it may be the result of methodological error such as erroneous morphological interpretation or non-midshaft plane of section. Variability might also have an intraspecific origin, or an interspecific origin, with bones of similar morphologies belonging to different species.

Methodological origin – The low specialization, postulated paedomorphic character of postcrania and lack of an ontogenetic series of large Temnospondyli may lead to ambiguous taxonomic determination of unassociated postcranial elements (Pawley and Warren, 2004). Erroneous taxonomic assignment of these bones thus may be the origin of the problematic interpretations applied to these specimens. However, in the bones described here, the morphological features characteristic for each taxon are well preserved and their taxonomic affinities based on the morphology seems to be unequivocal (Case, 1911; Cope, 1878; Kissel, 2010; Miner, 1925; Pawley and Warren, 2006; Romer, 1957). Nevertheless, it is possible that more taxa than currently recognized are present in the locality.

The plane of section also might have an influence on the apparent histotype. Konietzko-Meier and Klein (2013) showed that the bone microstructure is highly variable within millimeters of the sampled region. The histological midshaft with the neutral zone (the area where growth started) is more locally restricted in plesiomorphic tetrapod long bones than the morphological midshaft. Different sampling planes thus may intersect a variable microstructure of the medullary region; the density of trabeculae increases proximally and distally together with decreasing cortical bone thickness. Laurin and Buffrénil (2015) documented the misinterpretation of lifestyle based on the microstructural features of *Ophiacodon* because the section plane was not precisely mid-diaphyseal. However, the specimens from Briar Creek Bonebed varied not only on the microstructural level, but also represent the different histology (growth pattern, tissue type, vascularization pattern), suggesting that the plane of section cannot explain all of the observed variability.

Intraspecific variability – There are a number of reasons for a high intraspecific variability of bone microstructure; environmental fluctuations, developmental plasticity and different individual age, intraskeleton variability, various growth strategies, genetic variability, sexual dimorphism or other drastic changes in the life cycle (Woodward et al., 2014). Previously sampled anamniotic tetrapods that best demonstrate intraspecific histological variability are *Dutuitosaurus ouazzoui* (Steyer et al., 2004), *Metoposaurus diagnosticus* from Poland (Konietzko-Meier and Klein, 2013; Konietzko-Meier and Sander, 2013) and *Gerrothorax pulcherrimus* (Sanchez and Schoch, 2013).

The histological variant of the smallest *Eryops* ulna (IPBSH-76) may result from developmental immaturity. The cortex in the smallest ulna is histologically immature, representing histotype I (Fig. 3). However, because it is immature, it is possible that the vascular pattern may change during ontogeny. Even if histotype I, represented by the smallest ulna, only represents juvenile ontogenetic variation of *Eryops*, we still observe a discrepancy between the histology and morphology among other bones, which based on the morphology, can be assigned to a taxon and lack clear immature characters.

One of the potential explanations is environmental plasticity. Environmental plasticity has been documented in the bones of *Gerrothorax pulcherrimus*, where it is expressed

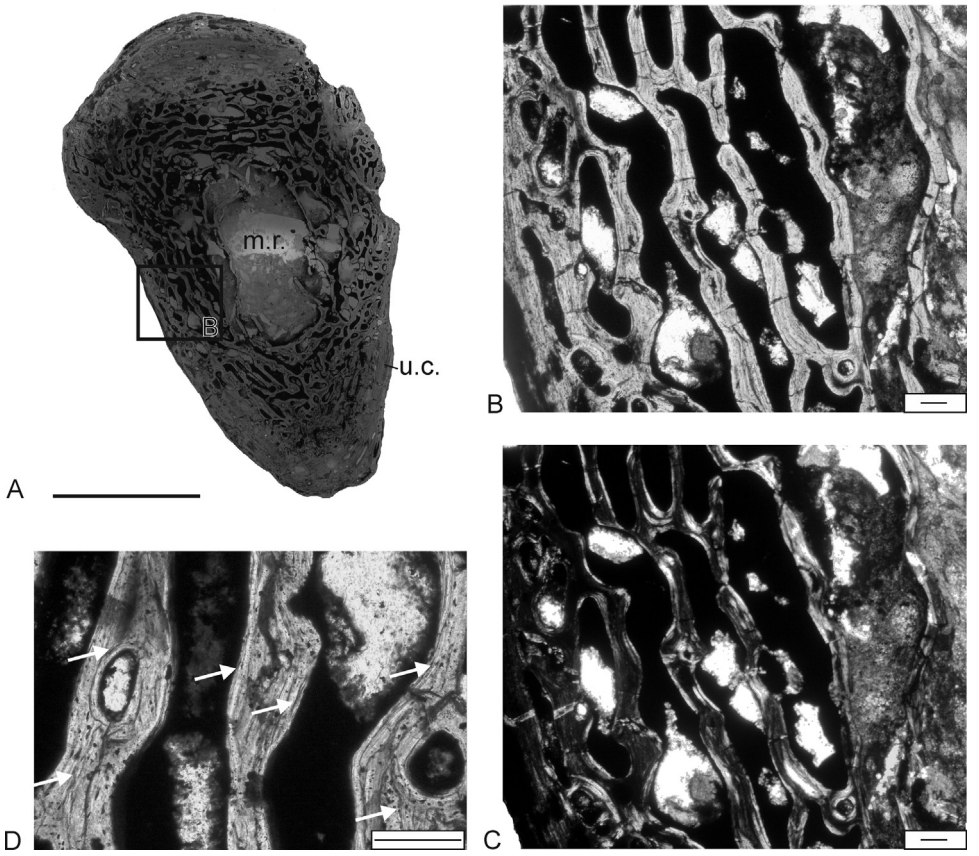

Fig. 7. Histotype V is represented by ulna IPBSH-74, which morphologically can be assigned to *Archeria*. A. Microanatomy of the midshaft; note the open medullary cavity. B. Fragment of the spongy cortex; note the thin layer of lamellar bone in outermost part of cortex, imaged in normal transmitted light. C. The same as B but in polarized transmitted light. D. Trabeculae enlarged with the resorption lines (white arrows). Scale bars equal 500 μm for A, and, 200 μm for B–D. Abbreviations: m.r.: medullary region; u.c.: unremodelled cortex.

Fig. 7. Histotype V représenté par l'ulna IPB-74, qui peut être assigné morphologiquement à *Archeria*. A. Microanatomie à de la diaphyse ; à noter la cavité médullaire ouverte. B. Fragment d'os spongieux ; à noter le feuillet mince d'os lamellaire dans la partie la plus externe du cortex, en lumière transmise normale. C. Idem B, en lumière transmise polarisée. D. Trabécules agrandis, avec les lignes de résorption (flèches blanches). Barres d'échelle = 500 μm pour A, et 200 μm pour B–D. D, Abréviations : m.r. : zone médullaire ; u.c. : cortex non remodelé.

as a variable growth rate, duration of juvenile period, age at maturity, and life span (Sanchez and Schoch, 2013). This variability is seen in sympatric and allopatric populations. Regardless, the bones of this taxon always demonstrate common histological features in tissue organization and general growth pattern (Sanchez and Schoch, 2013), in contrast to the intrageneric histological variability observed in the bones from the Briar Creek Bonebed.

One of the main problems with the histological sections studied here is the origin of histotype V, visible in two taxa and bones: *Eryops* radius and *Archeria* ulna. A possible scenario for the origin of this histotype is provided by the extensive cortical erosion that occurs during the development of *Gerrothorax* (Sanchez and Schoch, 2013). In the earliest stage, the cortex is very compact and composed of fibrous or parallel-fibered bone, occasionally crossed by some radial extrinsic fibers. Later in development, this cortex is deeply pierced by numerous bays of erosion and becomes lamellar in the periphery (Sanchez and Schoch, 2013). This suggests that our bones with a spongy structure (histotype V) may represent the late ontogenetic forms of one of the other histotypes (III or IV) visible in the femora and humeri (Fig. 7). However, it is not possible to determine which one with the data at hand.

The published histological studies of an *Eryops* femur (Sanchez et al., 2010 and Quémeneur et al., 2013) describe the microanatomy of this bone as highly spongy. This suggests that histotype V is characteristic of *Eryops*, especially if the radius (IPBSH-75) representing this histotypes morphologically belongs to this genus. Also, in the largest sampled *Eryops* femur (IPBSH-78) that displays histotype III, the shape of the erosion cavities is similar to those observed in spongy bones, in which osteoclast activity increases in the medullary and perimedullary regions. However, even in the largest femora (IPBSH-78), a clearly developed lamellar-zonal cortex is always present, contrary to histotype V.

Based on the histological framework, bones with histotype V may also belong to *Archeria*. The remnants of the primary tissue are still visible in the spongy cortex interstices between secondary osteons (Fig. 7C) and the lamellar bone. The outermost layer visible in histotypes V is similar

to those in histotype IV. This suggests that histotype V represents the late developmental stage of histotype IV, and all bones with histotypes IV and V, despite the strong morphological variations, belong to one taxon, which in this case is *Archeria.*

However, histotypes IV and V may represent adaptations to very different modes of life. Osteosclerosis observed in the histotypes IV may be produced by bone mass increase, which results in heavy, dense bone typical of slow swimmers living in shallow water (Canoville and Laurin, 2009; Houssaye, 2009; Laurin et al., 2009; Laurin et al., 2011; Ricqlès and Buffrénil, 2001). The spongy condition present in the histotypes V is characteristic of open marine active swimmers (Houssaye et al., 2013, 2014; Ricqlès and Buffrénil, 2001). Based on these observations, *Archeria* may present two opposite life strategies; pelagic, slow swimmer and active swimmer. Histotype IV confirms the traditional interpretation of *Archeria* as an aquatic, slow animal. Histotype V is closer to the hypothesis proposed by Laurin and Soler-Gijón (2010), which suggests a possible marine lifestyle in *Archeria*, though not necessarily pelagic.

This dual signal visible in the bones assigned to one taxon is plausible if the animal's mode of life changed during its life cycle. The ulnae, with histotypes IV and V, are very similar in size, and based on the morphology (ossification through the olecranon process), they seem to be at the same ontogenetic stage. The similarity in morphological stage excludes the slow, developmental origin of different histotypes IV and V and suggests a parallel development of described structures during the same ontogenetic stage.

The most drastic change in the mode of life during the life cycle of extant amphibians is associated with metamorphosis. The earliest known records of metamorphosis are based on morphological characters of Permo-Carboniferous dissorophoids (Schoch, 2009, 2014; Schoch and Fröbisch, 2006) and seymouriamorphs (Laurin, 2000). In Lissamphibia, metamorphosis is sometimes visible histologically as a metamorphosis line, which is a thick line close to the medullary region, but a transition from one histotype to another has not been observed (i.e. Ento and Matsui, 2002; Esteban et al., 1999, 2002; Hemelaar, 1988; Jakob et al., 2002; Khonsue et al., 2001, 2002; Montori, 1990; Olgun et al., 2001). However, as of yet the histological variation between the pre-metamorphic and post-metamorphic forms, not only for early stegocephalians, but also for lissamphibians, is unknown.

The remaining possibility is the parallel development of different microstructures throughout life history representing i.e. the sexual dimorphism. However, it is not possible to assess this cause of variability here because we lack data on the sex of the sampled individuals.

To understand the source of this variability requires further sampling of more ontogenetic series of other taxa.

Interspecific variability – Our initial histological studies of various temnospondyl intercentra suggested that temnospondyl bone histology may contain a taxonomic signal (Konietzko-Meier et al., 2014). We cannot exclude the possibility that several tetrapod taxa with similar bone morphologies, but different histotypes, are preserved in the Briar Creek Bonebed. This suggests either that the taxonomic diversity of the Briar Creek locality has been underestimated in the past, or that infraspecific histological variability in early limbed vertebrates was greater than currently recognized.

Acknowledgments

We wholeheartedly thank Jack and Marie Loftin of Archer City, Texas, for their help and hospitality in the field. Koen Stein (Steinmann Institute) and Herman Winkelhorst (Aalten, NL) provided assistance in the field. We thank Olaf Dülfer, Rebecca Hofmann, and Marlene Nowak for making the thin sections and Georg Oleschinski for photography (all Steinmann Institute). We extend our particular gratitude to the late Farish Jenkins Jr. and Jessica Cundiff (MCZ), Mark Norell and Carl Mehling (AMNH), Richard Cifelli, Jennifer Larson, and Kyle Davies (OMNH), Pamela Buzas-Stephens (MSU), Jeffrey Wilson and Gregg Gunnell (UMMP), William Simpson, Jörg and Nadia Fröbisch (FMNH) for access to collections. Finally, we thank the landowner of the Briar Creek Bonebed, Jeff Lindeman, for granting permission to excavate in 2010 and 2011. This project was funded by DFG grant SA 469/34-1 and the University of Bonn.

We thank the reviewers (A. Canoville, S. Sanchez and third anonymous reviewer) and editor (M. Laurin) for improving the text and for all constructive comments.

References

Canoville, A., Laurin, M., 2009. Microanatomical diversity of the humerus and lifestyle in lissamphibians. Acta Zool. 90, 110–122.

Case, E.C., 1911. A revision of the Cotylosauria of North America, 145. Carnegie Institution of Washington, Publication, pp. 1–122.

Case, E.C., 1915. Permo-Carboniferous red beds of North America and their vertebrate fauna, 207. Carnegie Institution of Washington, Publication, pp. 1–176.

Cope, E.D., 1878. Descriptions of extinct Batrachia and Reptilia from the Permian formation of Texas. P. Am. Philos. Soc. 17, 505–530.

Ento, K., Matsui, M., 2002. Estimation of age structure by skeletochronology of a population of *Hynobius nebulosus* in a breeding season (Amphibia, Urodela). Zool. Sci. 19 (2), 241–247.

Esteban, M., Garcia-Paris, M., Castanet, J., 1999. Bone growth and age in *Rana saharica*, a water frog living in a desert environment. Ann. Zool. Fenn. 36, 53–62.

Esteban, M., Sanchez-Herraiz, M., Barbadillo, L., Castanet, J., Marquez, Z., 2002. Effects of age, size and temperature on the advertisement calls of two Spanish populations of *Pelodytes punctatus*. Amphibia-Reptilia 23, 249–258.

Fischer, J., Schneider, J.W., Hodnett, J.P.M., Elliott, D.K., Johnson, G.D., Voigt, S., Joachimski, M.M., Tichomirowa, M., Götze, J., 2014. Stable and radiogenic isotope analyses on shark teeth from the Early to the Middle Permian (Sakmarian–Roadian) of the southwestern USA. Historical Biol. 26 (6), 710–727.

Francillon-Vieillot, H., Buffrénil, V. de, Castanet, J., Géraudie, J., Meunier, F.J., Sire, J.Y., Zylberberg, L., Ricqlès, A. de., 1990. Microstructure and mineralization of vertebrate skeletal tissues. In: Carter, J.G. (Ed.), Skeletal biomineralization: patterns, processes and evolutionary trends, Vol. I. Van Nostrand Reinhold, New York, pp. 471–530.

Hemelaar, A., 1988. Age, growth and other population characteristics of *Bufo bufo* from different latitudes and altitudes. J. Herpetol. 22, 253–388.

Houssaye, A., 2009. "Pachyostosis" in aquatic amniotes: a review. Integr. Zool. 4, 325–340.

Houssaye, A., Lindgren, J., Pellegrini, R., Lee, A.H., Germain, D., Polcyn, M.J., 2013. Microanatomical and histological features in the long bones of mosasaurine mosasaurs (Reptilia, Squamata) – implications for aquatic adaptation and growth rates. Plos One 8 (10), e76741.

Houssaye, A., Scheyer, T.M., Kolb, C., Fischer, V., Sander, P.M., 2014. A new look at ichthyosaur long bone microanatomy and histology: implications for their adaptation to an aquatic life. Plos One 9 (4), e95637.

Jakob, C., Seitz, A., Crivelli, A.J., Miaud, C., 2002. Growth cycle of the marbled newt (*Triturus marmoratus*) in the Mediterranean region assessed by skeletochronology. Amphibia-Reptilia 23, 407–418.

Khonsue, W., Matsui, M., Hirai, T., Misawa, Y., 2001. A comparison of age structures in two populations of the pond frog *Rana nigromaculata* (Amphibia: Anura). Zool. Sci. 18, 597–603.

Khonsue, W., Matsui, M., Misawa, Y., 2002. Age determination of Daruma pond frog, *Rana porosa brevipoda* from Japan towards its conservation (Amphibia: Anura). Amphibia-Reptilia 23, 259–268.

Kissel, R., 2010. Morphology, phylogeny, and evolution of Diadectidae (Cotylosauria: Diadectomorpha). University of Toronto Press, Toronto, 185 p.

Konietzko-Meier, D., Klein, N., 2013. Unique growth pattern of *Metoposaurus diagnosticus krasiejowensis* (Amphibia, Temnospondyli) from the Upper Triassic of Krasiejów. Poland. Palaeogeogr. Palaeoclimatol. Palaeoecol. 370, 145–157.

Konietzko-Meier, D., Sander, P.M., 2013. Long bone histology of *Metoposaurus diagnosticus* (Temnospondyli) from the Late Triassic of Krasiejów (Poland) and its paleobiological implications. J. Vertebr. Paleontol. 35 (5), 1–16.

Konietzko-Meier, D., Danto, M., Gądek, K., 2014. The microstructural variability of the intercentra among temnospondyl amphibians. Biol. J. Linn. Soc. 112, 747–764.

Labandeira, C.C., Allen, E.G., 2007. Minimal insect herbivory for the Lower Permian coprolite bone bed site of north-central Texas, USA, and comparison to other Late Paleozoic floras. Palaeogeogr. Palaeoclimatol. Palaeoecol. 247, 197–219.

Lamm, E.T., 2014. Preparation and sectioning of specimens. In: Padian, K., Lamm, E.T. (Eds.), Bone histology of fossil tetrapods, advancing methods, analysis, and interpretation. University of California Press, Berkeley, Los Angeles, London, pp. 35–54.

Laurin, M., 2000. Seymouriamorphs. In: Heatwole, H., Carroll, R.L. (Eds.), Amphibian biology. Surrey Beatty & Sons, Chipping Norton, pp. 1064–1080.

Laurin, M., 2004. The evolution of body size, Cope's rule and the origin of amniotes. Syst. Biol. 53 (4), 594–622.

Laurin, M., Reisz, R.R., 1995. A reevaluation of early amniote phylogeny. Zool. J. Linnean Soc. 113 (2), 165–223.

Laurin, M., Reisz, R.R., 1997. A new perspective on tetrapod phylogeny. In: Sumida, S., Martin, K. (Eds.), Amniotes origins: completing the transition to land. Academic Press, London, pp. 9–59.

Laurin, M., Soler-Gijón, R., 2010. Osmotic tolerance and habitat of early stegocephalians: indirect evidence from parsimony, taphonomy, paleobiogeography, physiology and morphology. In: Vecoli, M., Clément, G. (Eds.), The terrestrialization process: modelling complex interactions at the biosphere-geosphere interface. The Geological Society of London, London, pp. 151–179.

Laurin, M., Buffrénil, V. de, 2015. Microstructural features of the femur in early ophiacodonts: a reappraisal of ancestral habitat use and lifestyle of amniotes. C. R. Palevol (Early view).

Laurin, M., Canoville, A., Quilhac, A., 2009. Use of paleontological and molecular data in supertrees for comparative studies: the example of lissamphibian femoral microanatomy. J. Anat. 215, 110–123.

Laurin, M., Canoville, A., Germain, D., 2011. Bone microanatomy and lifestyle: a descriptive approach. C. R. Palevol 10, 381–402.

Marjanović, D., Laurin, M., 2013. The origin(s) of extant amphibians: a review with emphasis on the "lepospondyl hypothesis". Geodiversitas 35, 207–272.

Miner, R.W., 1925. The pectoral limb of *Eryops* and other primitive tetrapods. Bull. Am. Mus. Nat. Hist. 517, 145–312.

Montori, A., 1990. Skeletochronological results in thepyrenean newt *Euproctus asper* (Dugès, 1852) from one prepyrenean population. Ann. Sci. Nat. Zool. 11, 209–211.

Olgun, K., Miaud, C., Gautier, P., 2001. Age, size and growth of the terrestrial salamander *Mertensiella luschani* in an arid environment. Can. J. Zool. 79, 1559–1567.

Pawley, K., Warren, A., 2004. Immaturity vs. paedomorphism: a rhinesuchid stereospondyl postcranium from the Upper Permian of South Africa. Palaeontol. Afr. 40, 1–10.

Pawley, K., Warren, A., 2006. The appendicular skeleton of *Eryops megacephalus* Cope, 1877 (Temnospondyli, Eryopoidea) from the Lower Permian of North America. J. Paleontol. 80, 561–580.

Quémeneur, S., Buffrénil, V. de, Laurin, M., 2013. Microanatomy of the amniote femur and inference of lifestyle in limbed vertebrates. Biol. J. Linnean Soc. 109, 644–655.

Ricqlès, A. de., 1974. Recherches paléohistologiques sur les os longs des Tétrapodes V : Cotylosaures et Mésosaurs. Ann. Paleont. (Vert.) 60, 171–231.

Ricqlès, A. de, 1975. Recherches paléohistologiques sur les os longs des tétrapodes VII.1. Sur la classification, la signification fonctionnelle et l'histoire des tissus osseux des tétrapodes. Première partie. Ann. Paleont. 60, 171–216.

Ricqlès, A. de., 1978. Recherches paléohistologiques sur les os longs des tétrapodes VII – sur la classification, la signification fonctionnelle et l'histoire des tissus osseux des tétrapodes. Troisième partie, fin. Ann. Paleont. 64, 153–184.

Ricqlès, A. de, Buffrénil, V. de, 2001. Bone histology, heterochronies and the return of Tetrapods to life in water: where are we? In: Mazin, J.M., Buffrénil, V. (Eds.), Secondary adaptation of tetrapods to life in water. Verlag, München, pp. 289–310.

Romer, A.S., 1928. Vertebrate faunal horizons in the Texas Permo-Carboniferous red beds, 2801. University of Texas Bull, pp. 67–108.

Romer, A.S., 1947. Review of the Labyrinthodontia. Bull. Mus. Comp. Zool. 99, 1–368.

Romer, A.S., 1957. The appendicular skeleton of the Permian embolomerous amphibian *Archeria*. Contributions from the Museum of Paleontology, XIII (5). University of Michigan, pp. 103–159.

Ruta, M., Coates, M.I., Quicke, D.L.J., 2003. Early tetrapod relationships revisited. Biol. Rev. 78, 251–345.

Sanchez, S., Schoch, R.R., 2013. Bone histology reveals a high environmental and metabolic plasticity as a successful evolutionary strategy in a long-lived homeostatic Triassic Temnospondyl. Evol. Biol., http://dx.doi.org/10.1007/s11692-013-9238.

Sanchez, S., Germain, D., Ricqlès, A. de, Abourachid, A., Goussard, F., Tafforeau, P., 2010. Limb-bone histology of temnospondyls: implications for understanding the diversification of palaeoecologies and patterns of locomotion of Permo-Triassic tetrapods. J. Evol. Biol. 3 (10), 2076–2090.

Sander, P.M., 1987. Taphonomy of the Lower Permian Geraldine Bonebed in Archer County, Texas. Palaeogeogr. Palaeoclimatol. Palaeoecol. 61, 221–236.

Sander, P.M., 1989. Early Permian depositional environments and pond bonebeds in central Archer County, Texas. Palaeogeogr. Palaeoclimatol. Palaeoecol. 69, 1–21.

Schoch, R.R., 2009. The evolution of life cycles in early amphibians. Annu. Rev. Earth Pl. Sc. 37, 135–162.

Schoch, R.R., 2014. Amphibian evolution. The life of early land vertebrates. Wiley, New Jersey, 264 p.

Schoch, R.R., Fröbisch, N., 2006. Metamorphosis and neoteny: alternative developmental pathways in an extinct amhibian clade. Evolution 60, 1467–1475.

Shelton, C.D., Sander, P.M., Stein, K., Winkelhorst, H., 2013. Long bone histology indicates sympatric species of *Dimetrodon* (Lower Permian, Sphenacodontidae). Earth. Env. Sci. T. R. So. 103, 1–20.

Steyer, J.S., Laurin, M., Castanet, J., Ricqlès, A. de, 2004. First histological and skeletochronological data on temnospondyl growth: palaeoecological and palaeoclimatological implications. Palaeogeogr. Palaeoclimatol. Palaeoecol. 206, 193–201.

Woodward, H.N., Padian, K., Lee, A.H., 2014. Skeletochronology. In: Padian, K., Lamm, E.T. (Eds.), Bone histology of fossil tetrapods, advancing methods, analysis, and interpretation. University of California Press, Berkeley, Los Angeles, London, pp. 195–216.